HEFAT2011
8th International Conference on Heat Transfer, Fluid Mechanics and Thermodynamics
11 – 13 July 2011
Pointe Aux Piments, Mauritius

MODELLING HEAT AND MOISTURE TRANSPORT IN POROUS MATERIALS WITH CFD FOR BUILDING APPLICATIONS

Van Belleghem M.*[1], Ameel B.[1], Janssens A.[2], De Paepe M.[1]
*Author for correspondence
[1]Department of Flow, Heat and Combustion Mechanics,
Ghent University,
Ghent, 9000,
Belgium,
[2]Department of Architecture and Urban Planning,
Ghent University,
Ghent, 9000,
Belgium,
E-mail: marnix.vanbelleghem@ugent.be

ABSTRACT

Heat and moisture transport in buildings have a large impact on the building envelope durability, the energy consumption in buildings and the indoor climate. Nowadays HAM (Heat, Air and Moisture) models are widely used to simulate and predict the effect of these transport phenomena in detail.

Recently these HAM models are being coupled to CFD (Computational Fluid Dynamics) to study the moisture exchange between air and porous materials on a local scale (microclimates). A direct coupling approach between CFD and HAM is applied. The transport equations for heat and moisture in a porous material are directly implemented into an existing CFD package and the transport equations in the air and in the porous material are solved in one iteration by only one solver.

In this paper a model for moisture transport in the hygroscopic range and over-hygroscopic range is developed. This way a broad range of problems can be tackled such as drying phenomena and interstitial condensation in building components. The model is verified and validated with data from literature.

NOMENCLATURE

C	J/kgK	Specific heat capacity
C_b	kg/s³K⁴	Stefan-Boltzmann constant
d	m	thickness
D	m²/s	Water vapour diffusivity
E	J	Total energy
g	kg/m²s	Moisture diffusion flux
h	W/m²K	Convective heat transfer coefficient
h_m	kg/sm²	Convective mass transfer coefficient
K_l	s	Liquid moisture permeability
L	J/kg	Latent heat of evaporation
p	Pa	Pressure
Pr	-	Prandtl number
q_h	W/m²	Heat flux
R	J/kgK	Specific gas constant
RH	-	Relative humidity
Sc	-	Schmidt number
t	s	Time
T	K	Temperature
v	m/s	Velocity
w	kg/m³	Moisture content
x	m	Distance
Y	kg/kg	Water vapour mass fraction

Special characters

δ_a	s	Diffusion coefficient for water vapour in dry air
ε	-	Emissivity
λ	W/mK	Heat conductivity
μ	-	Water vapour resistance factor
ν	m²/s	Kinematic viscosity
ψ	-	Open porosity
ρ	kg/m³	density

Subscripts

air	Air
c	Capillary
cap	Capillary
e	environment
eff	effective
liq	Liquid
m	mass
mat	material
r	roof
s	surface
sat	Saturation
turb	Turbulent
va	Vapour in air
vap	Vapour

INTRODUCTION

Moisture in porous building materials can give rise to all kinds of damage phenomena such as frost

damage, salt crystallisation and mould growth. Also moisture in building envelopes can have a negative impact on insulation values and increase the energy use of buildings. Therefore a detailed knowledge of the moisture transport in these porous materials is important. Modelling the heat and moisture transport can help in understanding the mechanisms which are present.

In literature a lot of modelling approaches are found which can often be related to the work of Philip and de Vries [1] and Whitaker [2]. Philip and de Vries proposed a diffusion approach on a macroscopic level. This phenomenological approach considered the porous material as a continuous medium. Whitaker on the other hand made a more fundamental approach and started from the discrete phases in the porous material (solid, liquid, gas). He then averaged these equations to result again in a lumped model. Although this approach is more complex, it gives more insight in the porous material behaviour and the assumptions that are made during the modelling.

Different transported variables are used in the different transport models and generally two approaches can be found: a diffusivity approach and a permeability approach [3]. In the diffusivity approach the moisture content is used as the transported property while the permeability approach uses capillary pressure (which is related to the moisture content through the retention curve). Berger et al. [4] for example developed a numerical model for drying using a diffusivity approach. Examples of permeability approaches are found in [5,6].

The disadvantages however of these approaches are that they are difficult to couple directly with moisture transport in the surrounding air. Coupling with moisture transport in the air is often realised by using transfer coefficients. This approach lumps the effect of the heat and moisture boundary layer into one transfer coefficient which is often taken as a constant. Studies however showed that assuming a constant transfer coefficient can result in large errors [6,7]. Also these transfer coefficients are often difficult to determine experimentally and the analytical formulation found in literature do not always apply.

Computational Fluid Dynamics (CFD) solves the boundary layer directly. If the heat and moisture transport model could be coupled with CFD in a direct manner, there would be no longer a need for transfer coefficients. However, therefore the transported variable in the porous material has to be changed to a variable that is also transported in the air, to allow continuity.

In this paper the mass fraction of water vapour in air is proposed as the new transported variable for moisture transport. This variable is by default used in CFD for water vapour transport in the air. It is first investigated if this variable can be used to correctly simulate the vapour and liquid moisture transport in a porous material. The coupling of transport in the air and in a porous material is left for later studies and will not be discussed here.

HEAT AND MOISTURE MODEL

This section discusses the combined heat and moisture transport model in porous materials and air. Especially heat and moisture transport in porous materials is discussed since this is not generally incorporated in CFD packages.

This study focuses on porous materials that are capillary active. When looking at porous materials generally used in buildings, three phases will be present:

- Gas phase: air and water vapour
- Liquid phase: liquid water
- Solid phase: material matrix

In theory it is possible to model the different phases separately on a micro scale and subsequently integrate over the total material volume to obtain the macro scale heat and moisture transport [2]. This would however require such a detailed knowledge of the pore structure of the material that this approach is not feasible for materials encountered in practice. Therefore a phenomenological approach on a macro scale [1] was used for the derivation of the transport equations. In these transport equations the material is considered to be a continuum in which the 3 different phases overlap. By consequence macro heterogenic effects like cracks can not be simulated while the effects of micro heterogeneities are averaged over the calculation element.

Basically two conservation equations are deduced and solved: conservation of mass and conservation of energy. The conservative quantity for mass in the air is the water vapour density ρ_{vap} [kg/m³] (the amount of moisture contained in the air volume). The conserved quantity for mass in a porous material is the moisture content [kg/m³]. The conserved quantity for energy conservation is the total energy E [J]. First the moisture and energy transfer equations in air are deduced, then similar equations for a porous material are deduced.

Moisture transfer in air

Moisture is transported in air through a combination of convection and diffusion. In the air no liquid moisture is transported only water vapour. The water vapour diffusion flux is represented by g [kg/m²s] and is assumed proportional to the gradient of the water vapour density. D_{eff} is the sum of the molecular and turbulent vapour diffusion coefficient (equations (1)).

$$D_{eff} = D_{va} + D_{turb}$$
$$D_{va} = 2.31x10^{-5}\frac{101325}{p}\left(\frac{T}{273.16}\right)^{1.81} \qquad (1)$$
$$D_{turb} = \frac{\nu_{turb}}{Sc_{turb}}$$

In these equations D_{va} [m²/s] is the molecular diffusion coefficient and D_{turb} [m²/s] is the turbulent diffusion coefficient. p [Pa] is the operating pressure. The molecular diffusion coefficient is a property of the air-water vapour mixture only, while the turbulent diffusion coefficient is a property of the mixture and the flow. This turbulent diffusion coefficient is given as the ratio of the turbulent kinematic viscosity ν [m²/s]

to the turbulent Schmidt number Sc[-]. The Schmidt number represents the ratio of the kinematic viscosity to the mass diffusion coefficient. The value used for the turbulent Schmidt number is 0.7.

The water vapour density in the air can be represented as the product of mass fraction of water vapour in the air Y [$kg_{moisture}/kg_{air}$] and the total density of the air ρ_{air}.

$$\rho_{vap} = \rho Y \tag{2}$$

Equation (3) shows the transfer equation for water vapour in air in its divergence form. As mentioned before this transfer is governed by a convection term (second term on the left hand side) and a diffusion term (right hand side term). The first term on the left hand side represents the moisture storage in the air (moisture content change in time).

$$\frac{\partial(\rho Y)}{\partial t} + \nabla.(\vec{v}\rho Y) = -\nabla.\vec{g} = \nabla.(\rho D_{eff}\nabla Y) \tag{3}$$

Heat transfer in air

The heat transfer in the air can be represented by equation (4).

$$\frac{\partial(\rho CT)}{\partial t} + \nabla.[\vec{v}(\rho CT)] = \nabla.[\lambda_{eff}\nabla T - (C_{vap} - C_{air})\vec{g}T] \tag{4}$$

In this equation C [J/kgK] is the heat capacity with C_{vap} the heat capacity of water vapour and C_{air} the heat capacity of air. The mass weighted average heat capacity C is given by equation (5).

$$C = YC_{vap} + (1-Y)C_{air} \tag{5}$$

T [K] is the temperature, v is the air velocity and λ_{eff} [W/mK] is the effective heat conductivity. The effective heat conductivity is the sum of the molecular heat conductivity λ and the turbulent conductivity λ_{turb}. The turbulent conductivity is calculated from the turbulent kinematic viscosity and the turbulent Prandtl number with equation (6).

$$\lambda_{turb} = \rho C\frac{\nu_{turb}}{\mathrm{Pr}_{turb}}$$
$$\lambda_{eff} = \lambda + \lambda_{turb} \tag{6}$$

Similar to equation (3) three terms can again be distinguished: a storage term, a convective term and a diffusive term. Equation (4) includes the coupling between moisture transfer and heat transfer in the air. This is shown in the last term of the right hand side. Here the diffusion of moisture into a control volume is accompanied by the diffusion of air out of the control volume. Each diffusion flux is accompanied by an energy flux. The following values have been used for the different material properties: C_{vap}= 1875.2 J/kgK, C_{air}= 1006.43 J/kgK, λ= 0.0257 W/mK, Pr_{turb}= 0.85.

Moisture transfer in porous materials

To derive the transport equation for moisture in a porous material, the conservation equation for moisture content is again used as a starting point:

$$\frac{\partial w}{\partial t} = -\nabla.\vec{g} = -\nabla.(\vec{g}_{vap} + \vec{g}_{liq}) \tag{7}$$

Is this modelling approach it is assumed that moisture is transported in a porous material through two mechanisms: vapour transport and liquid moisture transport. Vapour transport is described by Fick's law:

$$\vec{g}_{vap} = -\frac{D_{va}}{\mu}\nabla\rho_{vap} \tag{8}$$

In this equation D_{va} [m²/s] is the molecular diffusion coefficient of water vapour in air, μ [-] is the water vapour resistance factor and is the ratio of the water diffusion coefficient of water vapour in still air to water vapour diffusion in the porous material.

This equation can be further rewritten as a function of temperature T and mass fraction Y using equation (2) and equation (9):

$$\rho_{air}(T,Y) = \frac{p}{T((1-Y)R_{air} + YR_{vap})} \tag{9}$$

Here p [Pa] is the operating pressure, R_a [J/kgK] is the specific vapour constant for air and R_v is the specific vapour constant for water vapour. R_{vap}=462J/kgK, R_{air}=286J/kgK. This results in equation (10).

$$\vec{g}_{vap} = -\frac{D_{va}}{\mu}\nabla(\rho_{air}Y) = -\frac{D_{va}}{\mu}\nabla\frac{pY}{T((1-Y)R_{air} + YR_{vap})}$$
$$= -\frac{D_{va}}{\mu}\rho_{air}\frac{R_a}{(1-Y)R_{air} + YR_{vap}}\nabla Y + \frac{D_{va}}{\mu}\rho_{air}\frac{Y}{T}\nabla T \tag{10}$$

Liquid moisture transport is described by Darcy's law:

$$\vec{g}_{liq} = -K_l\nabla p_c \tag{11}$$

Here K_l [s] is the liquid permeability and p_c [Pa] is the capillary pressure. Using Kelvin's law (12) and equations (13)-(15) [8] this transport equation can be rewritten in function of temperature T and mass fraction Y to have the same transported variables as before.

$$p_c = \rho_{liq}R_{vap}T\ln RH \tag{12}$$

$$RH = \frac{p_v}{p_{sat}} \tag{13}$$

$$p_{sat} = 611\exp\left(\frac{17.08(T-273.15)}{T-38.97}\right) \tag{14}$$

$$p_v = \frac{YpR_{vap}}{R_{air} + R_{vap}Y - R_{air}Y} \tag{15}$$

Substitution of equations (12) to (15) in equation (11) results in equation (16), which represents the liquid moisture flow rate in the porous material as a function of the temperature gradient and the mass fraction gradient. With the help of Kelvin's law the capillary pressure –which is usually the

transported variable for liquid moisture transport in porous materials – is translated to mass fraction.

$$\vec{g}_{liq} = -K_l \rho_{liq} R_{vap} \left[\begin{array}{l} \left(\ln RH + \dfrac{T}{RH} \dfrac{\partial RH}{\partial T} \right) \nabla T \\ + \dfrac{T}{RH} \dfrac{\partial RH}{\partial Y} \nabla Y \end{array} \right] \qquad (16)$$

The mass conservation equation can be further rewritten as a function of temperature T and mass fraction Y by introducing the moisture capacity. The moisture capacity gives the change in moisture content in the porous material for a change of the capillary pressure: $\partial w/\partial p_c$. Thus the first term of equation (7) can be expressed as:

$$\frac{\partial w}{\partial t} = \frac{\partial w}{\partial p_c} \frac{\partial p_c}{\partial RH} \frac{\partial RH}{\partial Y} \frac{\partial Y}{\partial t} + \frac{\partial w}{\partial p_c} \frac{\partial p_c}{\partial RH} \frac{\partial RH}{\partial T} \frac{\partial T}{\partial t} \qquad (17)$$

Substituting equations (10), (16) and (17) in equation (7) results in the total mass transfer equation for moisture transport in a porous material.

$$\begin{aligned} &\frac{\partial w}{\partial p_c} \frac{\partial p_c}{\partial RH} \frac{\partial RH}{\partial Y} \frac{\partial Y}{\partial t} + \frac{\partial w}{\partial p_c} \frac{\partial p_c}{\partial RH} \frac{\partial RH}{\partial T} \frac{\partial T}{\partial t} = \\ &\nabla . \left(\frac{D_{va}}{\mu} \rho_{air} \frac{R_{air}}{(1-Y)R_{air} + YR_{vap}} \nabla Y - \frac{D_{va}}{\mu} \rho_{air} \frac{Y}{T} \nabla T \right) \\ &+ \nabla . \left(\begin{array}{l} K_l \rho_{liq} R_{vap} \dfrac{T}{RH} \dfrac{\partial RH}{\partial Y} \nabla Y + \\ K_l \rho_{liq} R_{vap} \left(\ln RH + \dfrac{T}{RH} \dfrac{\partial RH}{\partial T} \right) \nabla T \end{array} \right) \end{aligned} \qquad (18)$$

Heat transfer in porous materials

No convective transport is assumed inside the porous material, only diffusion of moisture. This means that energy is only transported due to diffusion which results in equation (19).

$$\frac{\partial E}{\partial t} = \nabla . \vec{q}_h \qquad (19)$$

Here q_h is the total heat flux [W/m²]. This total heat flux has three contributions: a heat flux due to heat conduction in the porous material, a heat flux due to vapour diffusion though the porous material and a heat flux due to liquid moisture transport. The total energy E is the sum of the energy stored in the solid porous material matrix, the energy stored in the liquid moisture phase and the energy stored in the water vapour phase. Applying these assumptions to equation (19) results in the heat transfer equation for a porous material:

$$\begin{aligned} &\frac{\partial E}{\partial t} = \rho_{mat} C_{mat} \frac{\partial T}{\partial t} + w_{liq} C_{liq} \frac{\partial T}{\partial t} + w_{vap} C_{vap} \frac{\partial T}{\partial t} \\ &+ C_{liq} T \frac{\partial w_{liq}}{\partial t} + \left(C_{vap} T + L \right) \frac{\partial w_{vap}}{\partial t} \\ &= \nabla . \left[\lambda_{mat} \nabla T - C_{liq} T \vec{g}_{liq} - \left(C_{vap} T + L \right) \vec{g}_{vap} \right] \end{aligned} \qquad (20)$$

In this equation λ_{mat} [W/mK] is the heat conductivity of the porous material. This conductivity is a function of the moisture content of the porous material since moisture contained inside the porous material would result in an increase of the conductivity. ρ_{mat} [kg/m³] is the density of the porous material and C_{mat} is the heat capacity of the porous material. L is the latent heat of evaporation and is taken as a constant (2.5e6 J/kg). C_{vap} and C_{liq} are the heat capacities of vapour and liquid water respectively and are again assumed constant (C_{vap}= 1875.2 J/kgK, C_{liq}= 4192.1 J/kgK).

The total moisture content w [kg/m³] can by divided into the liquid moisture content w_{liq} and the vapour moisture content w_{vap}. Both are linked with the total moisture content through the open porosity ψ.

$$\begin{aligned} w_{liq} &= \frac{\psi - \dfrac{w}{\rho_{vap}}}{\dfrac{1}{\rho_{liq}} - \dfrac{1}{\rho_{vap}}} \\ w_{vap} &= \frac{\dfrac{w}{\rho_{liq}} - \psi}{\dfrac{1}{\rho_{liq}} - \dfrac{1}{\rho_{vap}}} \end{aligned} \qquad (21)$$

More details on how this model is implemented in a commercial available CFD solver (Fluent®) are found in [9].

VERIFICATION OF VAPOUR TRANSPORT MODELLING IN A POROUS MATERIAL

Verification of the model is necessary to check if the equations are implemented in a correct way. Different approaches to verify a model are found in literature. One way of verification is an inter model comparison were different model of different developers are compared. An other way is to compare the numerical results with an analytical solution. Milly et al. [10] presented such a solution to a vapour transport problem. Comparison of the analytical solution with the numerical results makes the verification possible.

The considered test case of Milly et al. [10] represents the one dimensional, coupled diffusion of heat and water vapour in a 10 cm high porous material. Initially the temperature in the material is 20°C and the relative humidity is 23.45%. A step change is imposed at the top of the material: the relative humidity changes to 27.11% while the temperature at the top is maintained at 20°C. This causes water vapour to diffuse into the porous material and leads to a varying temperature inside the material (due to latent heat release). The bottom of the material is considered to be vapour tight and adiabatic.

To obtain an analytical solution for this test case the following assumptions have to be made: (1) the transfer of sensible heat by vapour diffusion and the storage of sensible heat in the liquid water and the water vapour are negligible, (2) the perturbations in temperature and vapour density are so small that the relation between the moisture content (w) and the relative humidity (RH) can be considered linear around the initial state with all other material properties considered constant. If these assumptions are valid the analytical solution

developed by Cranck [11] can be used to describe the coupled heat and water vapour diffusion. The following material properties are used: w= 4.615RH + 74.261 [kg/m3]; D/μ= 4.37e-6 [m2/s]; $C\rho_{mat}$= 2e6 [J/m3K]; λ_{mat}= 1.5 [W/mK]. Note that a high heat capacity is chosen to guarantee small changes in temperature and hence assure the linear nature of the transport equations.

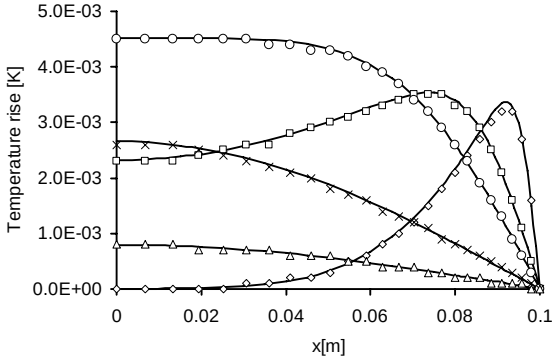

Figure 1 Verification for transport equations in the porous material when only vapour transport is present. Comparison at different times between the increase in temperature predicted by the analytical model (-) and the numerical model (◊: 500s, □: 5000s, ○: 20000s, x: 200000s, Δ: 500000s)

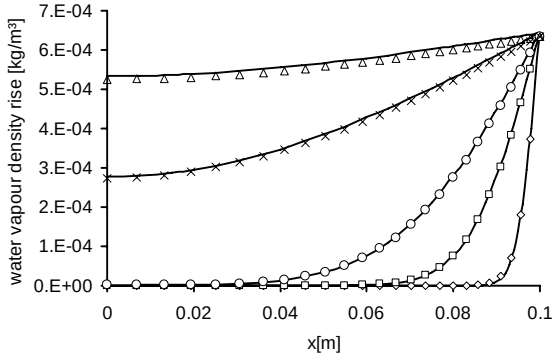

Figure 2 Verification for transport equations in the porous material when only vapour transport is present. Comparison at different times between the increase in water vapour density predicted by the analytical model (-) and the numerical model (◊: 500s, □: 5000s, ○: 20000s, x: 200000s, Δ: 500000s)

Figure 1 and Figure 2 respectively give the increase of the vapour density and the temperature inside the porous material, as predicted by the analytical and numerical model. Figure 1 shows that the increased water vapour density at the top of the material (x = 0.1m) results in a diffusion flux into the material until the water vapour density reaches the new level fixed at the top. Figure 2 shows how the water vapour diffusion into the material triggers a temperature increase which levels out in time under influence of the heat conduction to the surface. The excellent agreement between the analytical solution and the numerical results shows that the transport equations for water vapour in porous media have been correctly implemented and that the interaction between heat and water vapour transport is accurately represented.

The current model was also extensively validated. For that experimental results from Talukdar et al. [12] and Van Belleghem et al. [13] were used. The experiments of Talukdar were performed in a wind tunnel and measured the response of gypsum board on a step change of the relative humidity. The measurements of Van Belleghem et al. were performed in a climate chamber and measured the response of calcium silicate plate to a step change in relative humidity. The model gave good agreement with these measurements although it was found that it is very sensitive to the measured material properties [14]. More details on the validation of the vapour transport model are found in [9,13]

VALIDATION OF LIQUID MOISTURE TRANSPORT MODELLING

Experimental case

To validate the liquid moisture transport model, a drying experiment found in literature was used [6]. In this experiment described by Defraeye, a sample of ceramic brick is installed in a small wind tunnel. Dimension of the wind tunnel and the brick sample are indicated on Figure 3. For specific details on the wind tunnel setup the reader is referred to [6]. In this paper only a short description is given.

In the rectangular wind tunnel, air enters with a fully developed turbulent profile. This profile was measured with PIV (particle image velocimetry) and used as input for a CFD model of the wind tunnel. From this CFD model the convective heat transfer coefficient h [W/m²K] was estimated. The convective mass transfer coefficient was calculated through the Chilton-Colburn analogy [15]. Temperature near the brick sample was monitored at different locations (indicated by an X on Figure 3). For this paper the measurement results of three location were used: temperature at 10mm depth, 20mm depth and 30mm depth. The sample of ceramic brick was well insulated as indicated on the figure with extruded polystyrene (XPS) and all sides of the brick except one were made impermeable for moisture. The wind tunnel was located inside a climate chamber were the air was preconditioned to 23.8°C and a relative humidity of 44%. The porous brick was unsaturated at a moisture content slightly below the capillary moisture content, namely at 97% off w_{cap}. The material properties of the test material are listed in Table 1.

Table 1 material properties of ceramic brick

Property	Value	Unit
Density ρ_{mat}	2087	kg/m³
Heat capacity C_{mat}	840	J/kgK
Conductivity λ_{mat}	1+0.0047w	W/mK
Dry vapour resistance factor μ	24.79	-
Capillary moisture content w_{cap}	130	kg/m³

Other material properties that are needed in the model are the vapour diffusivity D [m²/s], the moisture retention curve w(pc) and the liquid permeability Kl [s]. These are given by

equations (22)-(24). From the vapour diffusivity the water vapour resistance factor can be determined.

$$D = \frac{2.61e-5}{\mu_{dry}} \frac{1-\left(w/w_{cap}\right)}{0.503\left(1-\left(w/w_{cap}\right)\right)^2+0.497} \quad (22)$$

$$w(p_c) = w_{cap}\left[\begin{array}{l} 0.846\left(1+\left(1.394e-5p_c\right)^4\right)^{-0.75} + \\ 0.154\left(1+\left(0.9011e-5p_c\right)^{1.69}\right)^{-0.408} \end{array}\right] \quad (23)$$

$$K_l = \frac{1.1437e-9}{\left(1+\left(-1.76e-5p_c\right)^{4.3}\right)^{1.6}} \quad (24)$$

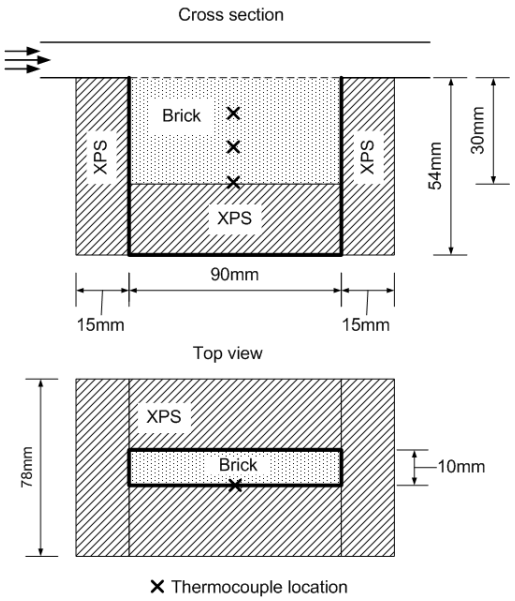

Figure 3 Schematic representation of the experimental setup. Cross section of wind tunnel and top view.

Numerical modelling approach

Figure 4 shows the schematical representation of the computational model for the HAM (Heat, Air, Moisture) modelling. Only a cross section of the brick sample is simulated. The insulation on the walls is incorporated into the boundary conditions. Measurements and simulations performed by De Fraeye [6] showed that the heat transfer coefficient on the side walls and bottom could be estimated at 8W/m²K. The thermal conductivity of the XPS was measured to be 0.034W/mK. Side walls and bottom were assumed to be impermeable for moisture. This resulted in the following heat flux boundary condition for the side walls and the bottom:

$$q_h = \frac{1}{\frac{1}{h}+\frac{d}{\lambda}}\left(T_e - T_s\right) \quad (25)$$

Here λ [W/mK] is the heat conductivity of the XPS; d [m] is the thickness of the insulation (0.02m at the bottom, 0.03m at the sides); h [W/m²K] is the heat transfer coefficient; T_e is the temperature of the surroundings (23.8°C) and T_s is the surface temperature. q_h is the heat flux through the boundary [W/m²].

At the top a mass flux is imposed, simulating the drying of the porous material. The boundary conditions at the top are given by:

$$\vec{q}_h = h\left(T_e - T_s\right) + Lh_m\left(Y_e - Y_s\right) + \frac{C_b}{\frac{1}{\varepsilon_r}+\frac{1}{\varepsilon_s}-1}\left(T_r^4 - T_s^4\right) \quad (26)$$

$$\vec{g} = h_m\left(Y_e - Y_s\right) \quad (27)$$

Here h is the convective heat transfer coefficient at the top which as already mentioned was calculated through CFD simulations and was estimated to be 22.5W/m²K. the convective mass transfer coefficient h_m was taken as 0.023kg/sm². The second term of equation (26) represents the latent heat leaving the computational grid. Here Y_e is the mass fraction of water vapour in the surrounding air (corresponding to 44%RH and 23.8°C) and Y_s is the mass fraction at the surface. The third term on the right hand side is the heat flux due to radiation. C_b is the Stefan-Boltzmann constant (5.67e10-8kg/s³K⁴) and ε_r and ε_s are respectively the emissivity of the roof and the brick surface (ε_r=0.97, ε_s=0.93). The brick is initially at 21.7°C.

The grid used in these simulations had in total 600x20 cells and was very fine near the top surface.

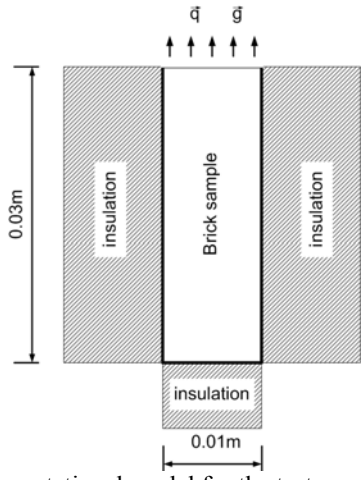

Figure 4 Computational model for the test case of Defraeye [6]. 2D cross section of the ceramic brick, side walls and bottom impermeable and insulated, on top heat and mass flux.

Isothermal modelling

A simplified modelling approach would be to simulate isothermal drying. This means that temperature changes inside the material are neglected. However this would result in a strong overestimation of the drying rate. Convective drying of a material is accomplished by evaporation of water from the material. However for this evaporation energy is needed. This results in a decrease of the temperature in the material. Due to this temperature decrease, the saturation vapour pressure and thus the saturation mass fraction at the surface of the porous material will decrease. This results in a lower driving force (mass fraction difference between surroundings and surface) at the surface and thus a lower mass flux and drying rate. This

decrease of the drying rate is not captured in the isothermal model. Therefore non isothermal modelling should be applied.

Non-isothermal modelling

The coupled heat and moisture problem is solved in this model in a segregated way. Within one iteration first the mass equation is solved and then the energy equation. The mass transport equation is simplified by assuming the material properties independent of the temperature. They are evaluated at the initial temperature of 21.7°C.

Figures 5, 6 and 7 show a comparison of the simulation results for temperature with the measurement at 10mm, 20mm and 30mm. Five cases were simulated using the 2D cross section model of the brick. The five cases differ in the boundary conditions that were used. Table 2 shows a list of the boundary conditions.

Table 2 simulated cases

Case	h [W/m²K]	λ XPS [W/mK]	h total bottom [W/m²K]	h total sidewall [W/m²K]
1	22.5	0.034	1.4	1
2	25	0.034	1.4	1
3	22.5	0.08	2.67	2
4	22.5	0.034	3.5	3.5
5	22.5	0.034	5	5

All calculated cases show the characteristics which are well known from experiments reported in literature [4,16]. After an initial decrease of the rate of drying (see Figure 8), the drying process enters the constant rate period (CRP). The CRP continues as long as the liquid flux to the surface from within the porous material can compensate for the rate of evaporation at the surface. If this is no longer the case, the drying process enters the falling rate period (FRP). During the FRP water is transported to the surface through vapour diffusion which is much slower than liquid moisture transport. This explains the rapid decrease of the drying rate after the CRP in Figure 8.

Figure 9 shows the evolution in time of the moisture content profile in the brick. The moisture content in the brick is initially 126.38kg/m³ which corresponds to a 97%w_{cap}. During the CPR the moisture content in the brick decreases rapidly across the entire profile. If the surface is dried out, the moisture content decreases much slower. A moisture front develops in the porous brick and slowly moves into the material.

Table 2 lists the 5 cases that were simulated. Case 1 is the reference case with boundary conditions taken from Defraeye [6]. Temperature inside the porous material starts at the initial value and then drops due to the evaporation of moisture as seen in Figure 5-7. During the CRP, the temperature remains low. If the surface of the brick starts to dry out and liquid moisture no longer reaches the surface, moisture transport is dominated by vapour diffusion to the surface. Since less vapour evaporates from the surface, the temperatures start to rise again. From Figures 5-7 it is clear that case 1 underestimates the temperatures in the brick sample. At the same time the duration of the CRP is overestimated. The simulations shows a CPR up to 6 hours were the measurements only show a CPR of less than 4 hours. A more detailed study of the boundary conditions is needed to explain some of the deviation between measurements and simulation.

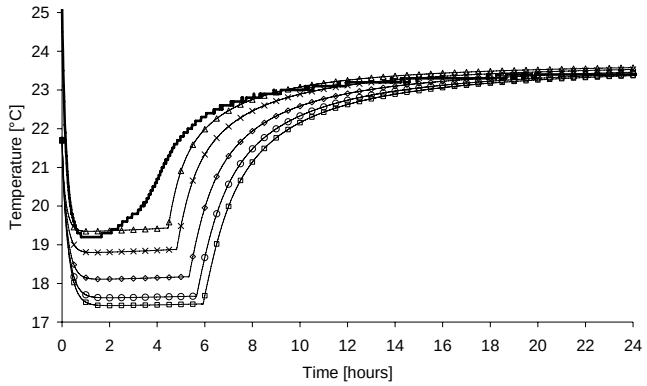

Figure 5 Temperature in the ceramic brick at a depth of 10mm. Comparison of simulation and measurement (case 1 □, case 2 ○, case 3 ◊, case 4 x, case 5 Δ)

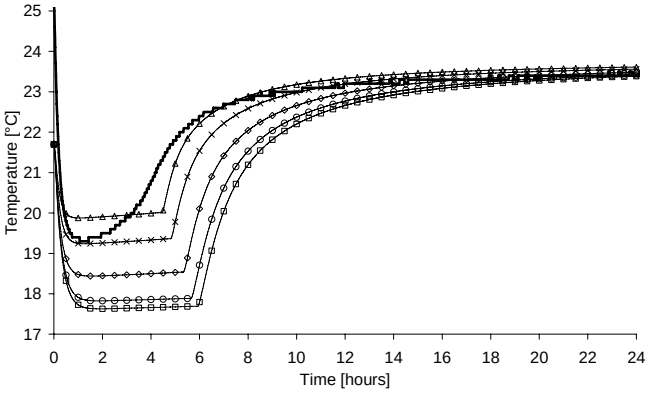

Figure 6 Temperature in the ceramic brick at a depth of 20mm. Comparison of simulation and measurement (case 1 □, case 2 ○, case 3 ◊, case 4 x, case 5 Δ)

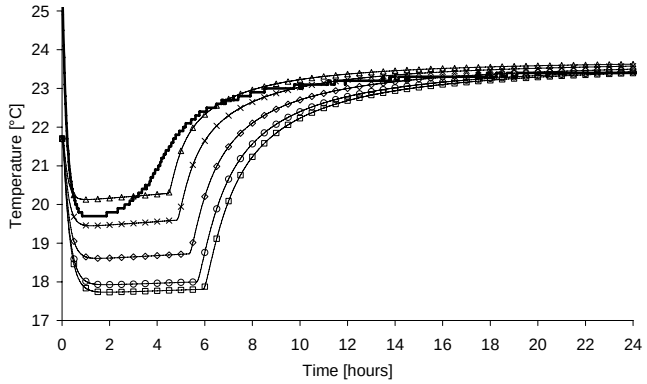

Figure 7 Temperature in the ceramic brick at a depth of 30mm. Comparison of simulation and measurement (case 1 □, case 2 ○, case 3 ◊, case 4 x, case 5 Δ)

EFFECT OF BOUNDARY CONDITIONS AND MATERIAL PROPERTIES ON MOISTURE TRANSPORT MODELLING RESULTS

Four extra cases derived from case 1 (reference case) were proposed the study the effect of the boundary conditions on the simulations results. In case 2 the heat transfer coefficient was increased from 22.5W/m²K to 25W/m²K. The simulations show that the temperature inside the porous material increases as expected. However the temperature increase is limited and does not explain the deviations with the measurements.

In cases 3-5 the insulation boundary conditions are altered. For case 3 only the thermal conductivity of the insulation was altered from 0.034W/mK to 0.08W/mK, while for cases 4 and 5 the entire transfer coefficient was altered (increased). These simulations show that a higher heat flux at the boundary walls would result in a better fit of the simulations with the measurements. Due to the higher heat flux, a higher temperature inside the porous material is reached. This results in a higher temperature at the surface of the material and thus a higher drying rate during the CRP since the saturation mass fraction at the surface increases with increasing temperature. A higher drying rate results in a shorter CRP. This is also shown in Figure 8. The best results are found for a transfer coefficient of 3.5W/m²K at the side walls and bottom (case 4).

Note however that the sensitivity of the simulations to boundary conditions are probably not the main reason of deviations with measurements. Other factors which were also discussed by Defraeye [6] have an impact on the results. First of all the 3D effect were not taken into account in the current model. A 3D simulation would give more accurate results.

Secondly, since only a 2D cross section is simulated, the transfer coefficients are assumed constant along the length of the sample. In reality however a boundary layer will developed over the sample and heat and mass transfer will be larger in the beginning of the sample. This results in a 3D moisture distribution in the porous material which is not captured here.

Finally also the material properties can have a significant impact on the results. Sensitivity analysis in previous studies revealed the importance of hygrothermal properties like liquid permeability and moisture retention curve [6,14].

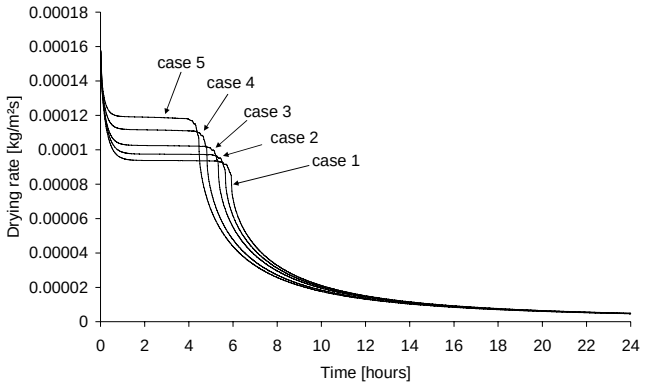

Figure 8 Drying rate for simulation cases 1-4

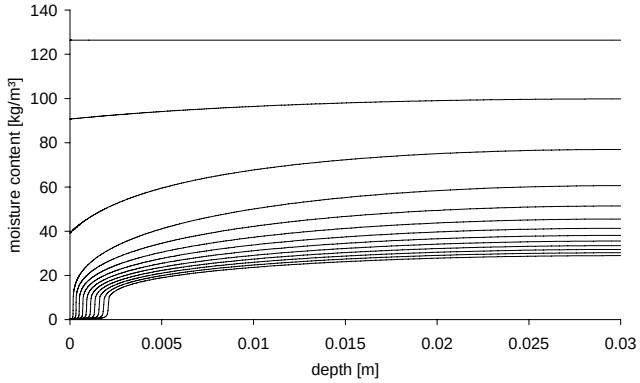

Figure 9 Moisture profiles during drying of brick sample (case 5). The time between subsequent profiles is 2 hours.

CONCLUSION

This paper describes the development of a coupled CFD-HAM model. In previous studies CFD was already successfully used to model coupled heat and vapour transport in porous materials, in this study it is investigated if CFD can be coupled to a liquid moisture transport model in a direct manner. Therefore the mass fraction of water vapour in air was introduced as the transported variable.

For this newly developed model first the vapour transport modelling was verified using an analytical case developed by Milly et al. [10]. Further validation of the model was performed using experimental data from Talukdar et al. [12] and Van Belleghem et al. [13].

Validation of the coupled heat and liquid moisture model was performed using experimental data produced by Defraeye [6]. In this experiment the drying of a sample of ceramic brick was studied and temperature evolutions inside the sample were measured.

It was found that the current model is able to capture all well known drying phenomena such as the different drying phases (constant drying rate period CRP, falling rate period FRP). However no perfect match was found between the model and the measurements. The study showed that the boundary conditions have a large impact on the modelling outcome and it was concluded that the deviations between measurements and model are probably due to a wrong estimation of the boundary conditions and due to the simplified 2D modelling approach. Future study should reveal if a more detailed 3D modelling approach with spatially varying convective transfer coefficients would result in a better agreement with the measurements.

ACKNOWLEDGMENT

The results presented in this paper have been obtained within the frame of the research project IWT-SB/81322/VanBelleghem funded by the Flemish Institute for the Promotion and Innovation by Science and Technology in Flanders. Its financial support is gratefully acknowledged.

REFERENCES

[1] Philip, J.R., de Vries, D.A., Moisture movement in porous materials under temperature gradients, *Transactions of the American Geophysical Union,* Vol. 38, 1957, pp. 222-232

[2] Whitaker, S., Simultaneous heat, mass and momentum transfer in porous media: A theory of drying, Academic Press, New York, 1977.

[3] Carmeliet, J., Roels, S., Determination of the Isothermal Moisture Transport Properties of Porous Building Materials, *Journal of Thermal Envelope and Building Science*, Vol. 24, No. 3, 2001, pp. 183-210

[4] Berger, D., Pei, D.C.T., Drying of hygroscopic capillary porous solids - a theoretical approach, *International Journal of Heat and Mass Transfer,* Vol. 16, 1973, pp. 293-302

[5] Janssen, H., Blocken, B., Carmeliet, J., Conservative modelling of the moisture and heat transfer in building components under atmospheric excitation, *International Journal of Heat and Mass Transfer,* Vol. 50, No. 5-6, 2007, pp. 1128-1140

[6] Defraeye, T., Convective Heat and Mass Transfer at Exterior Building Surfaces, Ph.D. thesis, KULeuven, Leuven, 2011, 334 pp.

[7] Steeman, H.-J., Janssens, A., Carmeliet, J., De Paepe, M., Modelling indoor air and hygrothermal wall interaction in building simulation: Comparison between CFD and a well-mixed zonal model, *Building and Environment,* Vol. 44, No. 3, 2009, pp. 572-583

[8] Hens, H., Building Physics – Heat, Air and Moisture, *Ernst & Sohn*, Berlin, 2007

[9] Steeman, H.-J., Van Belleghem, M., Janssens, A., De Paepe, M., Coupled simulation of heat and moisture transport in air and porous materials for the assessment of moisture related damage, *Building and Environment,* Vol. 44, No. 10, 2009, pp. 2176-2184

[10] Milly, P.C.D., Moisture and heat transport in hysteretic, inhomogeneous porous media: a matrix head-based formulation and a numerical model, *Water Resources Research,* Vol. 18, No. 3, 1982, pp. 489-498

[11] Cranck, J., The mathematics of diffusion, *Clarendon press*, Oxford, 1975

[12] Talukdar, P., Olutmayin, S.O., Osanyintola, O.F., Simonson, C.J., An experimental data set for benchmarking 1-D, transient heat and moisture transfer models of hygroscopic building materials. Part I: Experimental facility and material property data, *International Journal of Heat and Mass Transfer*, Vol. 50, No. 23-24, 2007, pp. 4527-4539

[13] Van Belleghem, M., Steeman, M., Willockx, A., Janssens, A., De Paepe, M., Benchmark experiments for moisture transfer modelling in air and porous materials, *Building and Environment,* Vol. 46, No. 4, 2011, pp. 884-898

[14] Van Belleghem, M., Steeman, H.-J., Steeman, M., Janssens, A., De Paepe, M., Sensitivity analysis of CFD coupled non-isothermal heat and moisture modelling, *Building and Environment*, Vol. 45, No. 11, 2010, pp. 2485-2496

[15] Chilton, T.H., Colburn, A.P., Mass Transfer (Absorption) Coefficients Prediction from Data on Heat Transfer and Fluid Friction, *Industrial and Engineering Chemistry,* Vol. 26, 1934, pp. 1183-1187

[16] Landman, K.A., Pel, L., Kaasschieter, E.F., Analytic modelling of drying of porous materials, *Mathematical Engineering in Industry*, Vol. 8, No. 2, 2001, pp. 89-122